Advances in Engineering Research : Possibilities and Challenges
ISSN Print: 3079-5192
ISSN Online: 3079-5206
https://doi.org/10.63313/AERpc.9048

Study on micro-hole morphology of Ni-based superalloy optimized by pulse-delay dynamic modulation of nanosecond laser

Xuecheng Gao[1,2]. Shufeng Sun[1,2,*]. Jin Wang[1,2*]. Fengyun Zhang[1,2]. Yaofei Ma[1,2]. Tao Wei[1,2]. Junbao Li[1,2] and Pingping Wang[1,2]
[1]Discipline Innovation and Wisdom Introduction Base of High-end Laser Intelligent Manufacturing Technology and Equipment, school of Mechanical and Automotive Engineering, Qingdao University of Technology, Qingdao 266520, China
[2]Key Laboratory of High-end Laser Manufacturing Technology and Equipment of Shandong Province, school of Mechanical and Auto-motive Engineering, Qingdao University of Technology, Qingdao 266520, China
Email: sunshufeng@qut.edu.cn

How to cite this paper: Gao, X. C., Sun, S. F., Wang, J., Zhang, F. Y., Ma, Y. F., Wei, T., Li, J. B., & Wang, P. P. (2025). Study on micro-hole morphology of Ni-based superalloy optimized by pulse-delay dynamic modulation of nanosecond laser. Advances in Engineering Research: Possibilities and Challenges, 2(2), 44-53. ISSN Print: 3079-5192; ISSN Online: 3079-5206.
https://doi.org/10.63313/AERpc.9048
Published: 2025-08-25

Abstract

Ni-based superalloys are widely used in aerospace for their excellent high-temperature properties.. To address thermal damage and dimensional ac-curacy issues faced by IN718 in high-power nanosecond laser micro-drilling, this study proposes a pulse-time modulation strategy. By dynamically control-ling heat accumulation through precise pulse-delay adjustments, a segmented energy delivery mechanism enhances through-hole quality. Two pulse-delay op-timization strategies are proposed and verified in comparison with the con-ven-tional processing: the optimized hole size accuracy is improved by 70%, the av-erage roughness of the hole wall is reduced by 30%, and the taper of the through-hole is reduced by 54%.

Keywords

Nanosecond laser; Laser drilling; Pulse delay; Ni-based superalloy

1. Introduction

Ni-based superalloys are widely used in high-temperature service environments such as aero-engine turbine blades and gas turbine hot-end components owing to their excellent high-temperature strength, oxidation resistance, and corrosion resistance [1][2]. In these critical components, the machining quality of micro-hole structures (e.g.,film-cooling holes) directly affects their heat dissipation efficiency and service life. However, the high hardness, high melting point and low thermal conductivity characteristics of Ni-based superalloys render them challenging to machine materials [3]. Consequently, optimization and in-depth development of micro-hole machining techniques for Ni-based superalloys such as Inconel 718 is crucial.

In the past decade or so, many methods have been proposed to improve the quality of micro-hole laser processing, such as liquid-assisted laser drilling [4][5][6], electric-field-assisted laser drilling [7][8][9], magnetic-field-assisted laser drilling [10][11][12], and ultrasound-assisted laser drilling [13][14][15]. Chang et al. explored the effect of magnetic field on laser drilling, and proposed that the magnetic field has a constraining effect on the plasma generated in the process, and the results showed that magnetic-field-assisted laser drilling would produce a deeper drilling depth [12]. Zhang et al. proposed a composite water-assisted drilling method of spraying water film combined with backside flowing water, which utilizes the water flow to take away the residual heat generated in the laser processing to reduce the heat-affected zone to achieve high-quality machining [6].Fan et al. proposed a bi-directional ultrasound-assisted laser drilling technology, analyzed the coupling effect of laser drilling and ultrasound assistance, and concluded that vertical ultrasound can improve drilling efficiency and horizontal ultrasound can reduce debris adhesion [15]. With the increasing demands for quality and efficiency in micro-hole processing, a single energy field assisted method is often difficult to meet these processing requirements, so researchers have proposed a composite energy field assisted processing [16][17][18]. However, this approach involves complex processing conditions and is currently confined to the laboratory stage,making widespread application difficult.

This paper proposes a simple and efficient laser drilling optimization strategy: introducing fixed delay times between specific pulse trains to dynamically regulate thermal accumulation effects, thereby improving micro-hole quality in high hardness materials. The effects of two pulse-delay strategies, face-delay and line-delay, on micro-hole morphology are compared. The processing mechanism dominated by thermal relaxation is elucidated in the context of melt pool dynamics analysis. The ablation behavior of nanosecond laser is investigated from the perspective of modulation time to significantly enhance the micro-hole quality at low cost, which is expected to provide some reference value for the industrialized application of laser drilling in hard-to-machine materials.

2. Experimental design

2.1. Materials and equipment

The experimental material was Inconel 718 (20 mm × 20 mm × 1 mm), which is widely used in aircraft engine turbine blades. The main elements contained in this material are Ni, Cr, Fe, and Nb.This study employed a 1064 nm nanosecond laser processing platform equipped with an IPG ytterbium-doped pulsed fiber laser. The laser specifications include: maximum average power of 200 W, beam quality factor M2 < 1.3, pulse width of 100 ns, and repetition frequency of 20 to 2000 kHz. This fiber laser is suitable for processing a wide range of metals, polymers, and ceramics. Fig .1. shows a schematic of nanosecond laser processing. The infrared beam from the laser first passes through a collimating lens to generate a collimated beam, which is then directed via a mirror-based beam delivery system to a galvanometer system, which accurately deflects the beam direction according to the preset processing path, so that the beam is focusing onto the workpiece surface through an F-theta lens. The resulting focused spot diameter of the laser beam is about 64 μm.

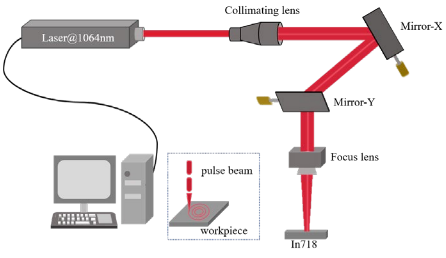

Figure 1. Schematic diagram of nanosecond laser processing

2.2. Experimental Methods

In conventional processing, nanosecond pulsed lasers are output at a fixed pulse repetition frequency (20 kHz) with no-delay as shown in Fig. 2. (a1), and pulsed lasers are output at a constant frequency, exhibiting a steady and sustained release of high energy as shown in Fig. 2. (a2), accompanied by a long period of energy accumulation. The laser pulse-delayed scanning drilling method introduces a delay time after each emission of a specified number of pulses, and then emits the next segment of pulses. By adjusting the inter-burst delay, the gap time between pulse groups is changed, which alters the mode of laser emission. This approach maintains the intra-pulse repetition rate, but controls the timing of the pulses to achieve precise control of the laser energy release and material removal time.

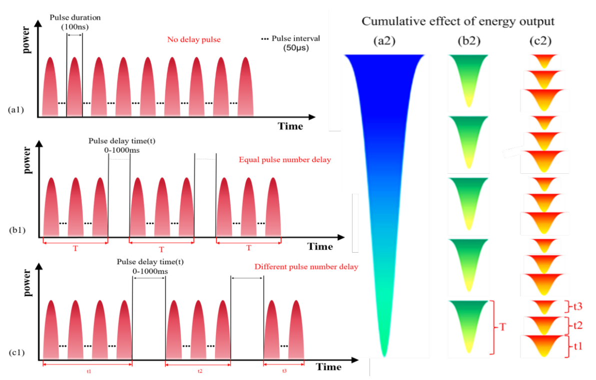

Figure 2. Schematic diagram of laser pulse delay action principle: (a) No delay; (b) Equal pulse number delay; (c) Unequal pulse number delay; (1) Pulse output schematic diagram; (2) Energy output cumulative effect diagram

Two delay strategies were implemented: Equal pulse number delay and unequal pulse number delay. Equal pulse number delay strategy as shown in Fig. 2. (b1), where a fixed delay time is set between each group of consecutive pulses. Each group contains an identical number of pulses with constant intra-burst intervals, resulting in periodic energy output is shown in Fig. 2. (b2). The unequal pulse number delay is shown in Fig. 2. (c1), Intra-burst intervals remain constant, but the number of pulses per group decreases progressively. Multiple pulse groups form a cycle with periodic repetition, and the number of pulses per group progressively decreases. The resulting energy output is shown in Fig. 2. (c2).

3. Results and discussions

3.1. Comparison of micro-holes with and without pulse-delay

In nanosecond laser processing, effective material removal primarily depends on the total cumulative laser energy input, which is determined by three key parameters: pulse count, pulse energy, and repetition frequency. In the case of no-delay, the number of pulses increases linearly with the processing time due to the fixed repetition frequency. And after the use of pulse-delay, the addition of delay time interval will directly affect the total processing time, mainly dependent on the length and number of the delay intervals. The number of pulses output per unit time without delay is greater than that with face-delay, which in turn is greater than that with line-delay. Specifically, in the no-delay state, the pulse output is continuous and stable, and the number of pulses per unit time is the largest; with face-delay introduces a fixed delay time between each set of pulses, and although the pulse frequency remains unchanged, the intervals between the pulse outputs increase the total machining time, resulting in a slightly lower number of pulses per unit time than in the no-delay state, with the number of pulse intervals determined by the number of times of machining operations, and the length of the time interval can be autonomously set. With line-delay, the number of pulse intervals is further increased, resulting in the slowest increase in the number of pulses, and therefore the lowest number of pulses per unit time, and the number of pulse intervals is determined by the fill spacing and the number of scans together.

As shown in Fig. 3., it is further verified by the change in the morphology of the entrance of micro-holes processed by nanosecond laser pulses ($2000 \sim 10^5$), when the number of pulses $\leqslant$ 2000, the laser action is not yet sufficient to form a through-hole, and the inner wall of the hole presents a molten state. At the initial stage of processing, the pulse energy is mainly used to destroy the metal film on the surface of the material, and the accumulation of energy is insufficient to remove the material effectively. In addition, the involvement of oxygen in the process induces the generation of oxides or cokes on the surface of the material, leading to the continuous accumulation of recast layers on the surface of the micro-hole, which seriously affects the smoothness and shape of the hole and makes it rough. This phenomenon is particularly significant in the no-delay and face-delay states, especially in the high pulse number conditions, the no-delay state of the orifice shows a clear protruding bowl, while the face-delay state does not form a clear protrusion, but the heat-affected zone expansion is serious, and both of them show a tendency of the outward expansion of the orifice, and surfaces of heat-affected zones or melting zones appear. In addition, the edge of the aperture is accompanied by a large number of splashes, because high-energy nanosecond laser irradiation melts the material to form a molten pool, and splashing occurs under the strong recoil pressure of the laser processing, and the molten material is solidified by the cooling effect of the air after the laser stops, resulting in the formation of solidified splashes.

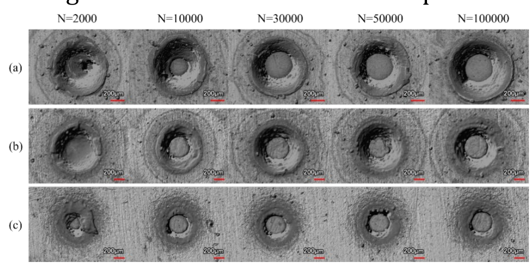

Figure 3. Comparison of micro-holes entrance morphology at different pulse numbers: (a) No delay state; (b) Surface delay state; (c) Line delay state

When the processing depth increases, the melt injection efficiency and drilling efficiency will decrease due to several reasons[19], and the molten metal solidifies at the sidewall or the bottom of the hole, leading to problems such as thickening of the recast layer, cracks, and porosity. In contrast, the line-delayed state can effectively suppress this phenomenon, with almost no expansion of the hole edge, a significant reduction in the heat-affected zone area, significantly less splashing, and a thinner recast layer, which suggests that the line-delayed strategy is able to optimize the mode of action of the laser energy and make the material removal process more uniform, thus enhancing the quality of micro-hole processing.

Fig. 4. demonstrates the three-dimensional micro-hole morphology maps for the three processing states at a laser pulse number N of 200000. The entrance diameter is the largest in the no-delay processing, close to 600 μm, which is about 200 μm wider than the design circle, and the exit diameter is larger in the no-delay state, followed by the face-delay, and the smallest exit diameter in the line-delay state, which are all relatively close to each other. In terms of hole wall taper, in the no-delay condition, the hole wall taper increases significantly due to the large inlet expansion range. In the line-delayed condition, the wall taper is minimized to as low as 2.89° due to the fine tuning of the pulse interval. Regarding the roundness of the holes, in the no-delay state, the hole wall is greatly affected by the thermal accumulation, resulting in an uneven hole shape and lower roundness. In the face-delayed state, the thermal effect is somewhat suppressed and the roundness of the hole is improved. In line-delayed processing, the hole shape is better due to the precise regulation of the pulse interval.

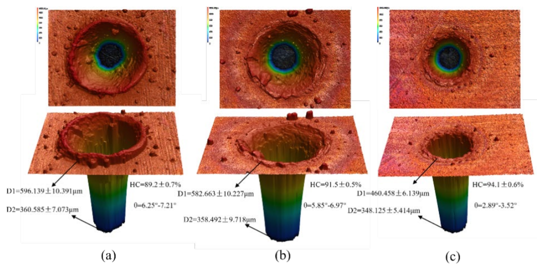

Figure 4. 3D morphology of micro-holes with pulse number N = 200,000: (a) No-delay state; (b) face-delay state; (c) Line-delay state

3.2. Mechanism analysis of micro-hole machining by laser line-delay processing

In order to further investigate the effects of material removal, melt flow and sputtering mechanism on the micro-hole morphology during laser line-delayed drilling, a systematic analysis and summary of the line-delayed processing mechanism was carried out by regulating the laser energy and the number of pulses, and the experimental results are shown in Fig. 5. .

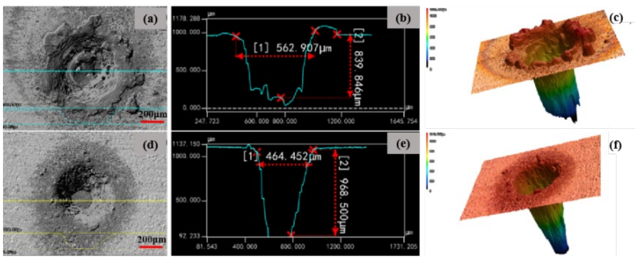

Figure 5. (a) Entrance morphology without delay; (b) Hole wall profile curve without delay; (c) 3D overall view of the micro-hole without delay; (d) Entrance morphology with line-delay; (e) Hole wall profile curve with line-delay; (f) 3D overall view of the micro-hole with line-delay;

As the number of processing times increases and the number of pulses increases, the cumulative effect enhances the heat input per unit area, and the micro-holes continue to expand and deepen. Meanwhile, in the process of melt pool formation and solidification, the material undergoes a liquid-solid phase transition, accompanied by solidification contraction effects, which compresses the local gas and produces violent recoil, thus inducing the formation of sputtered particles of different scales. The micro-hole morphology is most representative at 10 times of processing, and the no-delayed processing results are shown in Fig. 5. (a-c). There is a large amount of recast layer accumulation at the entrance of the holes, the diameter of the holes clearly exceeds the designed circular size, the lateral expansion of the micro-holes is obvious, and the machining depth is reduced. An irregular bump is observed at the bottom of the hole, indicating that the melt accumulates here during machining and concentrates on the machined side, forming a thick recast layer on the hole wall. In contrast, the line-delayed results, as shown in Fig. 5. (d-f), show minimal recast layer buildup at the entrance of the hole, greatly reduced lateral expansion of the micro-hole, accompanied by significant longitudinal expansion, and a significant increase in the machining depth compared to no-delay. At the same time, the hole walls show steeply stepped craters.

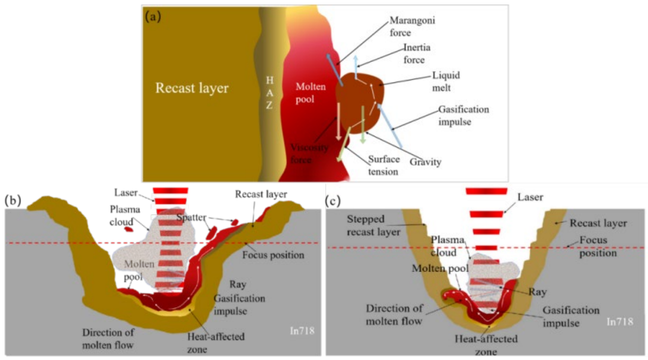

Figure 6. Melt pool dynamics analysis: (a) Local melt pool flow analysis; (b) No-delay; (c) Pulse-delay

Under laser irradiation, the material undergoes a four-phase transformation into a solid, a liquid, a gas and a plasma. Inelastic scattering between the incident photons and the material's electrons leads to a localized heat build-up, resulting in the formation of a flowing molten pool. Fig. 6. illustrates the flow characteristics of the molten pool. Initially, the laser is focused on the surface of the material and the energy shows a Gaussian distribution with the highest peak power in the center, and then gradually processed to a deeper layer with the increase of the number of pulses, and the melt in the hole will increases accordingly. As shown in Fig. 6(a). , during the material evaporation process, the recoil pressure acts on the bottom and sidewalls of the hole, driving the melt to flow upward along the hole wall [20]. At the same time, the temperature gradient at the liquid-gas interface triggers the thermocapillary force, i.e., the Marangoni effect, and the melt flow is also inhibited by surface tension and gravity, and the competition mechanism between multiple driving forces determines the final melt pool dynamic characteristics. In the case of uneven laser energy distribution, the locally lower instantaneous power prevents the recoil pressure from overcoming the surface tension and gravity, at which time a large amount of melt flows back to the bottom of the melt pool under the effect of gravity. Part of the melt is driven by the residual recoil pressure or inertial force to maintain upward flow, counteracting melt flows form a velocity shear layer at their junction, when the viscous force is weaker, the shear layer is destabilized and the formation of vortex, vortex through the enhancement of thermal convection and interfacial perturbation, significantly enhance the temperature gradient at the liquid-gas interface, which exacerbates the Marangoni effect [21].

Without delay as shown in Fig. 6. (b), the continuous output of the pulsed laser leads to excessive accumulation of heat, degradation of the melt pool composition , so that the apparent viscosity increases, the fluidity decreases, the material cannot be effectively removed, the melt reflux phenomenon is significant, and vortex effect leads to a large number of melt aggregated at the bottom of the crater, forming a thicker recast layer [22]. Melt reflux not only affects material microstructure, but also makes the processing rate show an initial rapid growth and then tend to level off. The increase of plasma and coalescing particles during the process results in the formation of a larger plasma cloud, which has a shielding effect on the laser beam and also prevents further processing in the longitudinal depth.And the evolution of the melt pool in the laser pulse-delay mode is shown in Fig. 6. (c). The high power density laser optimizes the material removal process by dynamically regulating the temporal and spatial distribution of energy through intermittent output, avoiding the thermal superposition effect of continuous pulsed laser. The intermittent heating allows the material to be cooled moderately at different stages, the volume of molten material is precisely controlled, and the material is rapidly removed mostly by vaporization or plasma sputtering. The presence of delay time makes the hole wall present a regular step-like structure, reduces the thermal stress gradient inside the material, and makes the defects mainly concentrated in the side wall and bottom of the hole. After the formation of the through-hole, with the increase of the number of machining times and axial feed, the defects generated in the early stage are gradually eliminated, which is conducive to the optimization of the micro-hole morphology. However, it is worth noting that the thickness of the recast layer will still exist eventually although the pulse interval is continuously extended, and the thickness of the recast layer will be reduced.

4. Conclusion

For laser drilling, a novel dynamic drilling strategy is proposed in this paper. The strategy realized the intermittent release of pulse energy by adjusting the delay time of infrared nanosecond laser pulses. Two different delayed scanning strategies line-delay and face-delay are experimentally designed and analyzed in comparison with the no-delay state. In addition, the mechanism of the line-delay strategy in micro-hole machining was investigated, and the machining parameters were optimized by using one-way factor analysis to finally obtain high-quality micro-hole morphology.

Pulse delay can regulate the time interval between pulse trains and achieves dynamic energy control. Among them, the line-delay strategy is superior to the face-delay and no-delay states, with less splashing on the micro-hole surface, thinner recast layer, no significant expansion of the orifice edge, and smaller heat-affected zone. The micro-holes in the line-delayed condition have the smallest inlet diameter of 460 μm, the lowest taper of 2.89°, the surface roughness of 4.27 μm, and the lowest longitudinal area roughness of 4.373 μm. In contrast, the inlet diameter of the non-delayed condition is close to 600 μm, which is about 200 μm larger than the design size.The pulse delay technology effectively reduces the content of oxygen elements in the processing and suppresses the occurrence of oxidation reaction. Due to the reduction of the local temperature gradient, the hydrodynamic behavior in the melting region tends to be stabilized, and the energy input of the laser to the hole wall is more uniform, which effectively reduces the internal roughness of the micro-hole and improves the topographic quality of the hole wall.

Acknowledgements

This work was supported by Qingdao University of Technology, Discipline Innovation and Wisdom Introduction Discipline lnnovation and Wisdom Introduction Base of High-end Laser Intelligent Manufacturing Technology and Equipment

References

[1] T. Zhang, H. Yuan, and M. Cai, Effects of recast layer on fatigue performance of laser-drilled holes in nickel-based superalloy, J. Mater. Process. Technol. 311, 117821 (2023)

[2] S. Ci, J. Liang, J. Li, et al., Optimizing process for pulsed laser additive manufacturing of nickel-based single crystal superalloy, Mater. Res. Express 10, 096511 (2023)

[3] K. Pang and D. Wang, Study on the performances of the drilling process of nickel-based superalloy Inconel 718 with differently micro-textured drilling tools, Int. J. Mech. Sci. 180, 105658 (2020).

[4] S. Duangwas, V. Tangwarodomnukun, and C. Dumkum, Development of an overflow-assisted underwater laser ablation, Mater. Manuf. Process. 29, 1226-1231 (2014).

[5] Y. Liu, H. Wang, Z. Zhang, et al., Laser-liquid composite micromachining technologies: a review of research progress, J. Adv. Manuf. Sci. Technol. 4, 2024002 (2024)Wright and Wright, W. (1906) Flying-Machine. US Patent No. 821393.

[6] R Zhang, H Zhang, R Ke,et al. Fabrication of high aspect ratio and low taper angle micro-holes utilizing complex water-assisted femtosecond laser drilling, Opt. Laser Technol. 185, 112608 .

[7] H. Wang and R. Li, Effect of process parameters and hybrid voltage-wind field on nanosecond laser spiral layer hole-cutting performance for thin stainless steel sheets, J. Manuf. Process. 135, 315-337 (2025).

[8] C. C. Ho and C. Y. Kao, Laser percussion drilling of transparent hard and brittle materials with ring-shaped electrodes, J. Manuf. Process. 101, 432-445 (2023).

[9] C. C. Ho and J. Y. Gao, Study on real-time detection of laser drilling in transparent hard and brittle materials by an external electric field, Meas. Sens. 18, 100147 (2021)

[10] C. Ye, G. J. Cheng, S. Tao, et al., Magnetic Field Effects on Laser Drilling, J. Manuf. Sci. Eng. 135, 061020 (2013).

[11] H. Wang, Y. Xu, J. Liu, et al., Magnet-assisted laser hole-cutting in magnesium alloys with and without water immersion, J. Manuf. Process. 61, 539-560 (2021).

[12] K. Kondo, T. Kanesue, J. Tamura, et al., Laser Plasma in a Magnetic Field, Rev. Sci. Instrum. 81, 02B716 (2010).

[13] S.-H. Alavi and S.-P. Harimkar, Ultrasonic vibration-assisted continuous wave laser surface drilling of materials, Manuf. Lett. 4, 1-5 (2015).

[14] D. Kang, P. Zou, W. Wang, et al., A lens ultrasonic vibration-assisted laser machining system for laser polishing and laser drilling of 304 stainless steel, Opt. Laser Technol. 144, 107419 (2021).

[15] Z. J. Fan,Z. M. Pei,Z. K. She, et al,Dual-directional ultrasonic vibration-assisted femtosec-

ond laser drilling of film cooling holes, Opt. Laser Technol. 180, 111484 (2025).

[16] K. Xia, N. Ren, Q. Lin, et al., Femtosecond laser drilling in superalloy with water-based magnetic assistance, Opt. Commun. 527, 128902 (2023).

[17] S. Amiri, M. Khajehzadeh, and M.-R. Razfar, Magnetic field and ultrasonic aided laser drilling effect on Ti6Al4V microstructural characteristics, Mater. Manuf. Process. 35, 1832-1841 (2020).

[18] H. Wang, Y. Xu, S. Zhu, et al., "Water-based helical laser hole-cutting in nickel super-alloy GH4049 assisted by longitudinal and transverse magnetic fields with/without ultrasonic assistance," Opt. Lasers Eng. 128, 105985 (2020).

[19] N. Shen, J. D. Bude, S. Ly, et al., Enhancement of laser material drilling using high-impulse multi-laser melt ejection, Opt. Express 27, 19864-19886 (2019).

[20] T. Zhang, L. Zhang, C. Zhang, et al., Physical study of spatter and melt pool dynamics during millisecond laser metals drilling, Opt. Commun. 482, 126627 (2021).

[21] C. Evrim, X. Chu, F. E. Silber, et al., "Flow features and thermal stress evaluation in turbulent mixing flows," Int. J. Heat Mass Transfer 178, 121605 (2021).

[22] Y. Zhang, Z. Shen, and X. Ni, Modeling and simulation on long pulse laser drilling processing, Int. J. Heat Mass Transfer 73, 429-437 (2014).